Unraveling BCR::ABL1-driven enhancer activation and transcriptional reprogramming in Ph B-ALL

Han Leng Ng
Centre for Haematology, Department of Immunology and Inflammation, Faculty of Medicine, Imperial College London, London W12 0NN, UK

Trudy Lee Glaser
Centre for Haematology, Department of Immunology and Inflammation, Faculty of Medicine, Imperial College London, London W12 0NN, UK

Mark E. Robinson
Center of Molecular and Cellular Oncology, Yale University, New Haven, CT 06511, USA

Kadriye Nehir Cosgun
Center of Molecular and Cellular Oncology, Yale University, New Haven, CT 06511, USA

Valeriya Malysheva
MRC London Institute of Medical Sciences, London W12 0NN, UK; Institute of Clinical Sciences, Faculty of Medicine, Imperial College, London W12 0NN, UK

Jintao Zhu
Centre for Haematology, Department of Immunology and Inflammation, Faculty of Medicine, Imperial College London, London W12 0NN, UK

Ozgen Deniz
Barts Cancer Institute, Queen Mary University of London, Charterhouse Square, London EC1M 6BQ, UK

Nicholas T. Crump
Centre for Haematology, Department of Immunology and Inflammation, Faculty of Medicine, Imperial College London, London W12 0NN, UK, and The Hugh and Josseline Langmuir Centre for Myeloma Research, Imperial College London, W12 0NN London, UK

Kaiyue Helian
Centre for Haematology, Department of Immunology and Inflammation, Faculty of Medicine, Imperial College London, London W12 0NN, UK

Andrew J. Innes
Centre for Haematology, Department of Immunology and Inflammation, Faculty of Medicine, Imperial College London, London W12 0NN, UK

Li Sun
Centre for Haematology, Department of Immunology and Inflammation, Faculty of Medicine, Imperial College London, London W12 0NN, UK

Mikhail Spivakov

MRC London Institute of Medical Sciences, London W12 0NN, UK; Institute of Clinical Sciences, Faculty of Medicine, Imperial College, London W12 0NN, UK

Markus Mueschen

Center of Molecular and Cellular Oncology, Yale University, New Haven, CT 06511, USA

Niklas Feldhahn

n.feldhahn@imperial.ac.uk

Centre for Haematology, Department of Immunology and Inflammation, Faculty of Medicine, Imperial College London, London W12 0NN, UK

Research Article

Keywords: BCR::ABL1, transcriptional deregulation, enhancer, P300/CBP, PROTAC, dependency

Posted Date: October 25th, 2024

DOI: https://doi.org/10.21203/rs.3.rs-5326686/v1

Additional Declarations: The authors declare no competing interests.

Abstract

B-lineage acute-lymphoblastic leukemia (B-ALL) is driven by genomic lesions and distinct transcriptional programs. Both are often directly linked as most B-ALLs are caused by genetic lesions at transcription factor (TF)-encoding genes. TFs largely mediate their function through gene regulatory 'enhancer' elements and enhancer deregulation is known to promote cancer initiation and progression. Consecutively, enhancer-targeting drugs are currently in clinical trials for advanced hematologic cancers such as acute myeloid leukemia and multiple myeloma. However, for B-ALLs not driven by TF-related genetic lesions it is largely unclear how their disease-promoting transcriptional programs are established, if it involves enhancer-deregulation, and if they would be sensitive to therapeutic enhancer-targeting.

We explore this here by focusing on Philadelphia chromosome-positive (Ph+) B-ALL, the most common B-ALL in adults with historically poor prognosis. Ph+B-ALL is driven by the BCR::ABL1 kinase, which has no TF-related function. We report that malignant transformation and associated transcriptional reprogramming by BCR::ABL1 is indeed accompanied by substantial enhancer activation and using Hi-C-based methods we connect enhancers to key genes in Ph+B-ALL. Consequently, Ph+B-ALL-specific enhancer signatures differentiate Ph+B-ALL from other leukemias. We further demonstrate that BCR::ABL1-induced enhancer activation depends on its kinase activity and is executed, at least in part, through the BCR::ABL1-activated TF STAT5. Highlighting the importance of enhancers and the potential of their therapeutic targeting, enhancer inhibition through CBP/P300-specific proteolytic degraders (PROTACs) effectively kills Ph+B-ALL cells.

Key Points

- BCR::ABL1-induced malignant transformation and transcriptional reprogramming towards Ph+B-ALL is defined by genome-wide enhancer activation.
- Enhancer-regulation affects key genes in Ph+B-ALL.
- Enhancer activation and associated chromatin interactions define Ph+B-ALL identity.
- Enhancer activation and associated chromatin interactions are regulated by BCR::ABL1 kinase activity and mediated through BCR::ABL1-activated TFs.
- Enhancer inhibition through CBP/P300-specific PROTACs effectively kills Ph+B-ALL cells.

Introduction

Acute-lymphoblastic leukemia (ALL) is the most common cancer and second most common cause of cancer-related death in children, and mostly arises from B-cell precursors (i.e., B-ALL). B-ALL subtypes are defined and driven by distinct initiating genetic lesions and disease-defining transcriptional programs[1,2]. Both are often directly linked, as most initiating genetic lesions in B-ALL affect transcriptions factor (TF)-encoding genes, which cause the disease-defining transcriptional program.

Indeed, 13/18 B-ALL subtypes [72%] with defined genetic alterations excluding iAMP21 and hyper/hypodiploidy are caused by lesions that alter one or two TFs[2]. TFs often mediate their function through enhancers, which are distal regulatory DNA elements located from a few kilobases up to 1.7 megabases away of the promoters they regulate[3-5]. Through physical interaction by DNA looping, enhancers, associated TFs, and epigenetic cofactors can regulate temporal-, spatial- and cell-type-specific activation of promoters. Importantly, elevated oncogene expression in cancer has been frequently attributed to aberrant enhancer function and many cancers are described to depend on 'enhancer reprogramming' or 'enhancer hijacking'[6-13]. Given the importance of transcriptional deregulation in cancer, enhancer-targeting drugs are explored as a therapeutic strategy for cancer treatment for the last two decades, with several improved drug candidates currently being in clinical trials for advanced and high-risk cancers including the hematological malignancies multiple myeloma (MM) and acute myeloid leukemia (AML) (e.g. NCT04068597, NCT03568656, NCT04575766, NCT05488548)[14,15].

Ph+B-ALL is the most common B-ALL in adults and historically a poor prognosis/high-risk leukemia[16]. Recent advances in replacing, supplementing, or consolidating chemotherapy with tyrosine kinases inhibitors and immunotherapy has improved its treatment outcome[17]. Nevertheless, relapses remain frequent and are associated with poor prognosis. Ph+B-ALL is driven by the oncogenic fusion gene *BCR::ABL1*, a constitutively active tyrosine kinase that activates its targets by phosphorylation. Multiple studies highlighted that Ph+B-ALL is defined by its distinct transcriptional program[1,2] causing upregulation of genes essential for disease initiation and progression[18-27]. However, how BCR::ABL1 induces this disease-defining transcriptional program is little understood. Likewise, it is unknown if disease development is caused by enhancer deregulation, and if Ph+B-ALL cells consecutively are sensitive to enhancer-targeting drugs.

While BCR::ABL1 has no TF-related function, it can induce activation or expression of TFs through phosphorylation. For example, BCR::ABL1 phosphorylates and thereby activates the signal-inducible TFs STAT1/3/5/6[28-30], of which STAT5[31], particularly STAT5B[32], was reported most important for Ph+B-ALL. Through STAT5, BCR::ABL1 further induces expression of *MYC*[18-20]. Additionally, BCR::ABL1 induces the RAS/MEK/ERK signaling pathway, thereby causing the expression of the ETS family TF, ETV5[21,33]. Other TFs with important function in B-ALL including Ph+B-ALL are MYB[34], CDK6[34], CDK8[35], FOXM1[36] and ERG[37]. However, it is unclear if they are induced by BCR::ABL1 and thereby shape the Ph+B-ALL-defining transcriptome, or if their importance reflects a general requirement in B-ALL cells. Likewise, it is unclear how BCR::ABL1 would coordinate their action and if it would involve enhancer deregulation.

To better understand how BCR::ABL1 establishes the Ph+B-ALL-defining transcriptional program, we adopted an integrative multi-omics approach to study the transcriptome, enhancer activities, and 3-dimensional interactions of enhancers with target genes in Ph+B-ALL cells. We performed an in-depth analysis of cells from human Ph+B-ALL patients and a murine Ph+B-ALL model using ChIP-Seq, RNA-Seq, and Hi-C-based methods to link enhancers to the promoters they regulate. We further interfered with

enhancer function to explore their role in Ph+B-ALL and investigated BCR::ABL1-regulated TFs that are recruited to them using targeted proteasomal degradation and knock-in models. Our results show that enhancer activation is a key characteristic of malignant transformation and transcriptional reprogramming by BCR::ABL1. We demonstrate that BCR::ABL1 itself causes their activation by coopting signal-induced TFs such as STAT5. Most importantly, we show that enhancer function is vital for Ph+B-ALL as their global inhibition using a CBP/P300-specific degrader (PROTAC) effectively kills Ph+B-ALL cells.

Methods

Cell lines and primary cells. All cell lines were obtained from the Deutsche Sammlung von Mikroorganismen und Zellkulturen (DSMZ, Germany). Human samples were deposited into, stored and subsequently retrieved from the Imperial College Healthcare Tissue Bank (ICHTB) under subcollection MEC_AR_16_030. All patients gave specific informed consent for the use of surplus tissue. Murine cells were processed as described[38,39] and experiments performed in agreement with ASPA guidelines & regulations and protocols approved by Home Office UK. Further information on culture conditions, processing, transfections and transduction can be found in the Suppl.Methods.

Drug treatments

Cells were treated with Ponatinib, AK-2292, dTAGV-1, A-485 or dCBP-1 as indicated in the figures/text and described in the Suppl.Methods using 1000X stocks and DMSO (Sigma) as control.

Next generation sequencing. ChIP-Seq, ATAC-Seq, RNA-Seq and PCHi-C were done as previously described[39-41]. Libraries were sequenced by paired-end sequencing at the MRC London Institute of Medical Sciences at Imperial College London or at Novogene. Further information on generation, processing and analysis can be found in the Suppl.Methods. Raw and processed data generated here can be found at Gene Expression Omnibus (GEO) under accession numbers GSE279589, GSE279594, GSE279643, GSE279644.

Western blot. Western blot was performed as previously described[39] using 4-15% Mini-PROTEAN TGX Precast Gels, the Mini-PROTEAN blotting system (Bio-Rad) and antibodies listed in the Suppl.Methods.

Flow cytometry. Cells were analyzed or sorted by flow cytometry using a BD LSRFortessa or SONY MA900 sorter, respectively, using the antibodies or fluorescent proteins as indicated in the figures and described in the Suppl.Methods.

Statistical analysis: Statistical analysis was performed using R or GraphPad PRISM 9/10 as indicated in the figures and Suppl.Methods.

Data Sharing Statement:

All NGS data generated here is available at GEO. Detailed information on protocols, methods and reagents can be found in the Suppl.Methods section within the Supplementary information. Any tools generated here (plasmids, cell lines etc) will be provided on request.

Results

BCR::ABL1-induced malignant transformation and transcriptional reprogramming is associated with genome-wide enhancer activation

To investigate if BCR::ABL1 causes enhancer deregulation to establish its transcriptional program, we first monitored BCR::ABL1-induced malignant transformation and associated transcriptional reprogramming for changes in enhancer activation. In detail, we used an established murine transformation model based on viral transduction of *ex vivo* cultured primary B-cell precursors (BCPs) with *BCR::ABL1*-encoding retrovirus[21,31,39,42] and monitored transcriptional changes and enhancer activation via RNA-Seq and H3K27ac ChIP-Seq. H3K27ac is a widely used histone marker of active regulatory regions including promoters and enhancers[43]. To differentiate between active promoters and active enhancers, we specifically analyzed H3K27ac signals at non-promoter regions. We first re-assessed RNA-Seq and H3K27ac ChIP-Seq data that we generated for a previous study[39] (Suppl.Fig.1A/B). In this study, BCPs from *53BP1*$^{-/-}$ mice were transduced with BCR::ABL1^{p210} (Fig.1A). Leukemic transformation was accompanied by substantial transcriptional reprogramming visualized by RNA-Seq (Fig.1B, left; Table S1). BCR::ABL1-induced genes included the known targets *Xbp1*, *Bcl2*, *Etv5*, *Dusp6* and *Ccnd2*, while downregulated genes included many with B-cell specific functions as described before[44]. Changes in gene expression were accompanied by changes in enhancer activation (Fig.1B, middle) including increased signals at the *Myc* super-enhancer in BCR::ABL1 expressing cells (Fig.1B, right). We repeated our setup using BCPs from C57BL/6 wild-type mice and BCR::ABL1^{p190}-encoding retrovirus (Suppl.Fig.1C/D; Table S2). This again showed that enhancer-deregulation occurs during BCR::ABL1-mediated transformation (Fig.1C). Of note, besides causing specific changes at defined sites, BCR::ABL1 induced a modest increase in H3K27ac, globally (Fig.1D).

Genes regulated by BCR::ABL1 and/or having critical functions in Ph+B-ALL are defined by long-range chromatin interactions with enhancers

To define which genes are enhancer-regulated in Ph+B-ALL, we performed promoter-capture Hi-C (PCHi-C)[41,45], which profiles long-range chromatin interactions of promoters with distal DNA regions (i.e., other ends/OE) such as enhancers. This is important as enhancers are often distally located to the promoters they regulate, sometimes being separated by megabases of DNA, and often do not regulate the most proximally located gene[3-5]. We integrated PCHi-C results with H3K27ac ChIP-Seq data to specifically define interactions between active promoters and active enhancers (Fig.2A). PCHi-C and H3K27ac ChIP-Seq were performed on two Ph+B-ALL cell lines and leukemia cells of one Ph+B-ALL patient that were *ex vivo* cultured on OP9 feeder cells (Suppl.Fig.2A-E). We identified ~55,000 significant long-range promoter

interactions per sample (CHiCAGO score >5) using probes for 18,202 protein-coding and 10,929 non-protein-coding genes. ~19% of these represented interactions of an H3K27ac+ active promoter with another H3K27ac+ distally located site (other end/OE), potentially indicative of an interaction with an enhancer (Fig.2A right, Table S3-8). In line with previous work[3,46], most active promoters were connected via long-range chromatin interactions to such distally located active regions (H3K27ac+ OEs), while the opposite was true for inactive promoters (Fig.2B), and active promoters with H3K27ac+ OE interactions displayed a much higher number of total long-range chromatin interactions compared to active promoters that only interacted with H3K27ac-negative OEs (Fig.2C). Notably, a fraction of active genes with H3K27ac+ OE interactions solely interacted with other active promoters (i.e., Promoter-Promoter Interactions/PPIs; 10.7%). However, most of them displayed interactions with H3K27ac+ non-promoter regions (i.e., potential Enhancer-Promoter Interactions/EPIs; 89.3%) either alone or in combination with PPIs (Suppl.Fig.2G). Interestingly, genes with EPIs, EPIs+PPIs, or PPIs appeared to serve different functions, with EPI+ only genes largely relating to signaling, EPI+PPI+ genes relating to gene expression and RNA processing, and PPI+ only genes associating with protein processing and transport (Suppl.Fig.2F). Importantly, while in total only 43% of all active genes displayed EPIs by PCHi-C (Fig.2D), these included many genes known to be regulated by BCR::ABL1 and/or having critical functions in Ph+B-ALL (Fig.2E), with several of them interacting with enhancers with crucial functions previously reported in other cancers[47-49].

To test whether the PCHi-C-defined genes with EPIs are indeed enhancer-regulated, we next inhibited the enhancer activator CBP/P300[50] in Ph+B-ALL cells with sub-lethal concentrations of A-485[51] and monitored resulting changes in gene expression by RNA-Seq. A-485 inhibits the histone acetylase activity of CBP/P300 reported crucial for CBP/P300-mediated enhancer activation[50] and causes dissociation of interacting enhancers and promoters[52] (Fig.2F) resulting in transcriptional downregulation of enhancer-regulated genes[52]. As such, we expected A-485 to cause preferential downregulation of PCHi-C-defined EPI+ genes compared to EPI- genes. In agreement with A-485 interfering with transcriptional activation, A-485 predominantly caused gene downregulation (~67% of DEGs; Table S9/10). Downregulated genes included EPI+ Ph+B-ALL key genes (Fig.2G and Suppl.Fig.2H) and lineage/cell type-specific genes as previously described[53] (Suppl.Fig.2I). A global analysis further showed that genes with PCHi-C-defined EPIs were indeed generally enriched for A-485-induced downregulation when compared to active genes without EPIs or PPIs (Fig.2H). Genes with PPIs rather showed a trend towards upregulation in response to A-485 (Fig.2H). Genes with both EPIs and PPIs showed a trend towards downregulation (Fig.2H), but this only reached statistical significance in one of the two cell lines tested (Suppl.Fig.J). The latter might relate to the opposite effect of A-485 on PPIs described here, which complicates the response of genes with EPIs+PPIs.

Together, the described results show that the transcriptional program of Ph+B-ALL is largely enhancer-associated and that BCR::ABL1-driven malignant transformation towards Ph+B-ALL is associated with defined changes in enhancer activation.

Enhancer activation and associated enhancer-promoter interactions define Ph+B-ALL identity

We next assessed if the changes in enhancer activity adapted by Ph+B-ALL cells are specific for this leukemia-subtype. We first assessed enhancer activation itself by comparing non-promoter H3K27ac ChIP-Seq signals present in Ph+B-ALL cell lines and primary leukemic cells to those from other leukemias and leukemia sub-types. H3K27ac signals at non-promoter regions clearly separated Ph+B-ALL from Ph-negative B-ALLs and BCR::ABL1-driven chronic myeloid leukemia (CML) by principal component analysis (PCA; Fig.3A). Likewise, we compared our PCHi-C data from Ph+B-ALL cells to PCHi-C data that we generated for healthy CD19+CD10+ BM BCPs and CML cells (Fig.3B/C). Specifically, we defined Ph+B-ALL 'core interactions' (i.e., EPIs and PPIs present in all three Ph+B-ALL samples; Suppl.Fig.3; Table S11) and assessed if these chromatin interactions would discriminate Ph+B-ALL cells from Ph-negative cells. Again, both, PCA and cluster analysis showed efficient separation of Ph+B-ALL cells from healthy BCPs and CML (Fig.3C). Notably, healthy BCPs clustered closer to Ph+B-ALL samples than CML and closer to primary Ph+B-ALL than to Ph+B-ALL cell lines, reflecting their similarities in lineage type and cellular state.

To validate these observations with a different method and samples, we performed HiChIP using H3K27ac antibodies[54] on leukemia cells from three patient-derived xenografts (PDX) each for Ph+B-ALL and *KMT2A::AFF1*+ B-ALL for comparison (Fig.3D-F). Like PCHi-C, H3K27ac HiChIP visualizes EPIs but, additionally, also visualizes enhancer-enhancer interactions (EEIs). In line with the above, H3K27ac HiChIP-defined EPIs and EEIs efficiently separated Ph+B-ALL from the *KMT2A::AFF1+* B-ALL cells (Fig.3E). We further compared H3K27ac HiChIP-derived EPI interaction scores per gene with RNA-Seq expression of the respective genes. Specifically, we used $\log_2$ fold change (log2FC) values from the comparison of Ph+B-ALL and *KMT2A::AFF1*+ B-ALL cells to assess if their separation by EPIs and enhancer activation relates to respective differences in their gene expression programs. The comparison indeed showed a trend towards positive correlation of EPIs and differential gene expression (Fig.3F).

Enhancer activity and enhancer-promoter interactions of BCR::ABL1-induced genes depend on BCR::ABL1 kinase activity

Of note, BCR::ABL1-induced transcriptional reprogramming and associated enhancer deregulation required a prolonged period of *BCR::ABL1* expression in our murine model (Fig.1), potentially indicating a positive selection for changes in enhancer function during malignant transformation instead of a BCR::ABL1-induced active process. To assess if BCR::ABL1 actively regulates enhancer activation, we thus inhibited BCR::ABL1 function for 24 hours using the tyrosine kinase inhibitor, Ponatinib, (Fig.4A) and monitored its effect on enhancer activation through H3K27ac ChIP-Seq. Ponatinib caused substantial loss of H3K27ac signals at H3K27ac+ non-promoter regions in both BCR::ABL1^{p190}-transformed murine BCPs and human Ph+B-ALL cells (Fig.4B). Ponatinib treatment also increased H3K27ac at other enhancer peaks, possibly reflecting resumed differentiation towards mature B-cells upon BCR::ABL1

inhibition as described previously[44,55]. Next, we specifically analyzed genes that display PCHi-C-defined EPIs (Fig.4C), focusing on genes that are downregulated upon Ponatinib treatment by RNA-Seq (Table S12-14). Inspection of the BCR::ABL1 target gene *CCND2* showed that PCHi-C interaction as well as H3K27ac signals at both promoters and enhancers were reduced upon Ponatinib treatment (Fig.4D). We consecutively analyzed all genes that are downregulated upon Ponatinib for changes in enhancer-promoter interactions, H3K27ac signals at promoters, and H3K27ac signals at interacting enhancers. PCHi-C scores and H3K27ac signals at both promoters and enhancers were indeed significantly reduced upon Ponatinib treatment in all cases (Fig.4E-G).

BCR::ABL1 induces enhancer activation in part through the BCR::ABL1-induced transcription factor STAT5

To define TFs that BCR::ABL1 employs to induce enhancer activation, we next assessed two published mass spectrometry data sets of BCR::ABL1 phosphorylation targets[56,57]. Within TFs identified by both studies, peptides of STAT family TFs dominated, including known phospho-tyrosine (pY) sites of STAT3, 5 and 6 important for their activation (Fig.5A). For the remainder, respective pYs were either not studied yet or shown functionally redundant (e.g. for NFYA^{Y266} ref.[58]). For functional analysis, we focused on STAT5B as it was reported the most important STAT in Ph+B-ALL[32], most enriched in our analysis (Fig.5A), known to recruit CBP/P300 to target genes[59], and linked by previous studies on murine B- and T-cells to enhancer activation[60,61]. Specifically, we generated a Ph+B-ALL cell line model that allows targetable proteasomal degradation (TPD) of STAT5 using the degron (dTAG) system[62,63]. In degron cells, a FKBP12^{F36V} tag is added to a protein of interest, which is a ligand for dTAG compounds that recruit E3 ligases to induce proteasomal degradation of FKBP12^{F36V}-tagged proteins. Through gene editing, we rendered both *STAT5A* alleles in Ph+B-ALL BV-173 cells nonfunctional and added an N-terminal FKBP12^{F36V} tag to *STAT5B* alleles (Fig.5B). Inclusion of an HA-tag further allow visualization of STAT5 by HA-ChIP-Seq. In parallel, we applied the novel STAT5A/B-specific degrader, AK-2292[64], on parental BV-173 cells with otherwise germline *STAT5A/B*. Of note, while dTAGV-1 addition was used in degron cells to induce STAT5 loss, in parental cells, which do not express FKBP12^{F36V}-tagged proteins, we used dTAGV-1 as a 'non-specific degrader' control (Fig.5C). With both systems, we achieved an almost complete loss of STAT5A/B (Fig.5C), though STAT5-degron cells exhibited reduced basal expression of STAT5, which was nevertheless further reduced by dTAGV-1 (Fig.5C). We first determined STAT5 binding through HA-ChIP-Seq using our STAT5-degron cells. STAT5-HA-bound sites included known canonical STAT5 targets (Fig.5D) and were highly enriched for STAT5 DNA-binding motifs (Fig.5E). In line with STAT5 being activated by BCR::ABL1 and phosphorylation being a prerequisite for DNA-binding[28-30], Ponatinib abolished STAT5-HA DNA-binding almost entirely (Fig.5D/F). STAT5 binding was further enriched at promoters of BCR::ABL1-regulated genes (821/1859 [44%] of all Ponatinib DEGs were STAT5-HA bound), which also displayed increased STAT5-HA signals compared to BCR::ABL1-unregulated genes (Suppl.Fig.4A/B). STAT5 loss through AK-2292 in parental cells or dTAGV-1 in degron cells likewise predominantly affected BCR::ABL1-regulated genes (125/187 [67%] of AK-2292 DEGs

overlap with Ponatinib DEGs; Fig.5G/H, Suppl.Fig.4C). In agreement with STAT5 also acting as a repressor[65,66], STAT5 loss induced both transcriptional downregulation and upregulation, with AK-2292 largely mirroring Ponatinib-induced transcriptional effects (Fig.5G right). However, notably, only 9% of genes (821/8705) with STAT5 at promoters overlapped with BCR::ABL1-regulated genes (i.e., Ponatinib DEGs, Suppl.Fig.4A), and STAT5 loss through AK-2292 only affected 7% (125/1859) of BCR::ABL1-regulated genes (Fig.5G left, Table S15/16).

Next, we applied these models to investigate STAT5 on BCR::ABL1-induced enhancer activation. Indeed, 69% of STAT5-HA peaks in untreated cells (17,059/24,642) did not overlap with a promoter, supporting a role of STAT5 in enhancer regulation in Ph+B-ALL. As we did not have PCHi-C data on BV-173 cells available, we defined enhancers as H3K27ac+ non-promoter regions within 50 kb proximity of each gene of interest, focusing on STAT5-HA-bound regions at AK-2292/Ponatinib-sensitive genes. AK-2292-induced loss of STAT5 in parental cells and dTAGV-1-induced STAT5 loss in degron cells indeed caused substantial reductions of H3K27ac at enhancers and promoters of the STAT5 target genes *CISH* and *SOCS1* (Fig.5I). Likewise, H3K27ac signals were reduced at STAT5-HA-bound enhancer regions when quantifying all AK-2292/Ponatinib-downregulated genes (Fig.5J). The opposite effect was observed for STAT5-HA-bound enhancers of AK-2292/Ponatinib-upregulated genes (Suppl.Fig.4D/E), and H3K27ac signals at promoters largely followed this trend (Suppl.Fig.4F/G).

Together, these results show that STAT5 function in Ph+B-ALL cells is largely dedicated to the regulation of BCR::ABL1 target genes, including the activation and repression of associated enhancers. However, its contribution to the BCR::ABL1-induced transcriptional program appeared surprisingly small, indicating that BCR::ABL1 employs additional TFs besides STAT5 for transcriptional reprogramming.

Therapeutic targeting of the enhancer-activators CBP/P300 causes cell cycle arrest and consecutive cell death of Ph+B-ALL cells

Given that key genes in Ph+B-ALL cells are enhancer regulated, we next wondered whether Ph+B-ALL cells are especially sensitive to CBP/P300 inhibition, which is essential for enhancer activation[50] as described before. Of note, CBP/P300 dependency had previously been described for leukemia and lymphoma cells[67]. However, B-ALL itself or individual B-ALL subtypes such as Ph+B-ALL had not been assessed in these studies. We therefore first assessed public DepMap[68] data, which defines cancer type-specific gene dependencies through negative Chronos/Ceres scores. This analysis showed that B-ALL indeed displays higher dependency for CBP and P300 compared to myeloid leukemia, T-cell leukemia and several B-cell lymphomas (Fig.6A, left), and that CBP/P300 dependencies further vary between individual B-ALL subtypes (Fig.6A, right). However, likely due to the generally low transduction efficiency of Ph+B-ALL cells with large CRISPR/Cas9 vectors that underlies Dependency Mapping[68], DepMap did not provide information on Ph+B-ALL cells. Therefore, we investigated CBP/P300 dependency of Ph+B-ALL cells ourselves experimentally using the recently developed CBP/P300-specific degrader/PROTAC, dCBP-1[67]. We chose dCBP-1 over A-485 here as we were not able to achieve complete H3K27ac loss with A-485 in Ph+B-ALL cells (Fig.2F), while dCBP-1 almost completely abolished CBP/P300-dependent

H3K27 acetylation (Fig.6B). Notably, dCBP-1 caused a marked G1 cell cycle arrest after 2 days of treatment (Fig.6C) and induced apoptosis in almost all Ph+B-ALL cells by day 5 of treatment (Fig.6D/E). Importantly, Ph+B-ALL cells showed similar sensitivity to dCBP-1 as multiple myeloma (MM) cells (Fig.6E), which so far were described the most CBP/P300-inhibition sensitive cancer cells[51,67] and for which CBP/P300-inhibitors are currently in clinical trials.

Discussion

Changes in enhancer activation are frequently linked to cancer initiation[13,69-71] and progression[72-76] and, as a result, enhancer inhibition is explored in many cancers as a therapeutic strategy, with BET inhibitors explored for the last two decades[15], and more specific CBP/P300 inhibitors currently in phase 1/2 clinical trials for treatment of high-risk cancers including AML, MM and advanced solid tumors[14]. We now demonstrate here that enhancer regulation is also a defining feature of the high-risk B-lineage leukemia Ph+B-ALL and that, in line with this, Ph+B-ALL cells are as sensitive to enhancer-targeting drugs as MM cells. Enhancer deregulation appears to be part of the process of malignant transformation towards Ph+B-ALL and is executed by its driving lesion, BCR::ABL1, itself for BCR::ABL1-regulated genes. Enhancer regulation also affects BCR::ABL1-unregulated genes, defining >40% of all active genes in Ph+B-ALL, likely contributing to the sensitivity of Ph+B-ALL cells to enhancer inhibition.

Of note, enhancer function has been studied in hematological malignancies such as AML, T-ALL and MM, and more recently also in B-ALL[75,76], but for B-ALL only as a collective group without differentiating between any subtypes. Thus, B-ALL subtype-specific dependencies on enhancer function remained unclear, in particular regarding B-ALLs not driven by altered TFs such as Ph+B-ALL. While we demonstrate this here now for Ph+B-ALL cells, we further show, by using H3K27ac ChIP-Seq, PCHi-C and H3K27ac HiChIP, that respective enhancer activation signatures and associated chromatin interactions further allow the distinction of Ph+B-ALL to other B-ALLs.

As BCR::ABL1 has no TF-related function, we investigated which TFs BCR::ABL1 uses to deregulate enhancer activation. Based on published mass spectrometry datasets on BCR::ABL1 phosphorylation targets, we focused on STAT5, as it was the most enriched. While STAT5 is an obvious candidate, as it is known to play a role in induction of BCR::ABL1-induced genes and STAT5 DNA-binding by ChIP-Seq was shown to be enriched at super-enhancers in murine B-cells[61]. However, the extent of STAT5 contribution to transcriptional deregulation by BCR::ABL1 in Ph+B-ALL remained unclear, in particular regarding BCR::ABL1-induced enhancer activation as the latter was not performed in human Ph+B-ALL cells and only a minority of STAT5-bound genes by ChIP-Seq were STAT5-regulated by RNA-Seq in this study[61]. To investigate STAT5 function, we used targeted proteasomal degradation, either through a PROTAC or a dTAG/degron model. In line with reported functions of STAT5 on gene expression in Ph+B-ALL and its association with enhancer function in other cell types, we show that STAT5 indeed mediates BCR::ABL1-induced gene deregulation and activation/suppression of associated enhancers. However, the contribution of STAT5 to BCR::ABL1-mediated changes was surprisingly mild (only 7% of BCR::ABL1-

regulated genes were STAT5-regulated), suggesting that BCR::ABL1 largely utilizes other TFs besides STAT5 to mediate its effect. It is worth to mention that most Ph+B-ALLs (83.7%) display deletions of the TF *IKZF1*[77], which modulates enhancer accessibility and gene expression[61,78]. However, as IKZF1 antagonizes STAT5-induced enhancer activation and gene expression[61], its loss should mostly have STAT5-promoting effects. Noteworthy are also the BCR::ABL1-phosphorylation targets STAT3 and STAT6. We did not investigate them here as previous reports indicated that BCR::ABL1-induced B-ALL primarily depends on STAT5[31,32]. However, these studies were done using murine models and mostly investigated dependencies, leaving the possibility that in human Ph+B-ALL, the full induction of the BCR::ABL1-induced transcriptional program requires STAT3/6 in addition to STAT5. Besides STAT proteins, ETS-related TFs such as ERG and ETV5 could further support the Ph+B-ALL-defining transcriptional program as both have been shown essential for Ph+B-ALL[21,33,37] and to modulate gene expression in these cells.

Together, while we did not define the complete set of TFs that mediate BCR::ABL1-induced enhancer activation, we show that therapeutic enhancer-targeting of hematologic malignancies could be extended to Ph+B-ALL. PROTACs against the enhancer activator CBP/P300 induce apoptosis in Ph+B-ALL similar to MM cells, for which CBP/P300 PROTACs are in clinical trials. Thus, while further studies are needed to explore the breadth of TF dependency for Ph+B-ALL, we define enhancer activation as a therapeutic vulnerability that could be explored in future treatments.

Declarations

Acknowledgements

The work was funded by Blood Cancer UK (BCUK, P77661, to NF) and The Blood Fund of the Imperial College Health Charity (PA2786 and PA6852, to NF). We thank the clinical staff of the Hammersmith hospital involved in providing patient samples, especially The John Goldman Centre for Cellular Therapy.

Authorship Contributions

HLN performed most experiments including PCHi-C, HiChIP, ChIP-Seq, RNA-Seq and respective bioinformatic analyses. TLG performed all dTAG experiments including RNA-Seq and ChIP-Seq and helped with dTAG knock-in generation. MER helped with processing and bioinformatic analyses of HiChIP data and RNA-Seq of mouse BCPs. KNC helped with processing of PDX samples for HiChIP. VM and MS helped with design and guidance for PCHi-C. JZ performed the GO analysis. OD performed ATAC-Seq. NTC provided guidance on dTAG experiments. KH helped with murine RNA-Seq experiments. LS helped with HiChIP analyses. AJI assisted with patient samples. MM supported HiChIP experiments and contributed to the manuscript. NF performed Western blots, flow cytometry, dTAG knock-in generation, mouse work, designed the study and wrote the manuscript.

Disclosure of Conflicts of Interest

The authors have no conflict of interest.

References

1. Harvey, R. C. *et al.* Identification of novel cluster groups in pediatric high-risk B-precursor acute lymphoblastic leukemia with gene expression profiling: correlation with genome-wide DNA copy number alterations, clinical characteristics, and outcome. *Blood* **116**, 4874-4884 (2010). https://doi.org:10.1182/blood-2009-08-239681
2. Gu, Z. *et al.* PAX5-driven subtypes of B-progenitor acute lymphoblastic leukemia. *Nat Genet* **51**, 296-307 (2019). https://doi.org:10.1038/s41588-018-0315-5
3. Javierre, B. M. *et al.* Lineage-Specific Genome Architecture Links Enhancers and Non-coding Disease Variants to Target Gene Promoters. *Cell* **167**, 1369-1384 e1319 (2016). https://doi.org:10.1016/j.cell.2016.09.037
4. Ray-Jones, H. & Spivakov, M. Transcriptional enhancers and their communication with gene promoters. *Cell Mol Life Sci* **78**, 6453-6485 (2021). https://doi.org:10.1007/s00018-021-03903-w
5. Schoenfelder, S. & Fraser, P. Long-range enhancer-promoter contacts in gene expression control. *Nat Rev Genet* **20**, 437-455 (2019). https://doi.org:10.1038/s41576-019-0128-0
6. Mansour, M. R. *et al.* Oncogene regulation. An oncogenic super-enhancer formed through somatic mutation of a noncoding intergenic element. *Science* **346**, 1373-1377 (2014). https://doi.org:10.1126/science.1259037
7. Groschel, S. *et al.* A single oncogenic enhancer rearrangement causes concomitant EVI1 and GATA2 deregulation in leukemia. *Cell* **157**, 369-381 (2014). https://doi.org:10.1016/j.cell.2014.02.019
8. Madisen, L. & Groudine, M. Identification of a locus control region in the immunoglobulin heavy-chain locus that deregulates c-myc expression in plasmacytoma and Burkitt's lymphoma cells. *Genes Dev* **8**, 2212-2226 (1994). https://doi.org:10.1101/gad.8.18.2212
9. Abraham, B. J. *et al.* Small genomic insertions form enhancers that misregulate oncogenes. *Nature communications* **8**, 14385 (2017). https://doi.org:10.1038/ncomms14385
10. Haller, F. *et al.* Enhancer hijacking activates oncogenic transcription factor NR4A3 in acinic cell carcinomas of the salivary glands. *Nature communications* **10**, 368 (2019). https://doi.org:10.1038/s41467-018-08069-x
11. Helmsauer, K. *et al.* Enhancer hijacking determines extrachromosomal circular MYCN amplicon architecture in neuroblastoma. *Nature communications* **11**, 5823 (2020). https://doi.org:10.1038/s41467-020-19452-y
12. Liu, T. *et al.* Enhancer co-amplification and hijacking promote oncogene expression in liposarcoma. *Cancer Res* (2023). https://doi.org:10.1158/0008-5472.CAN-22-1858
13. Montefiori, L. E. *et al.* Enhancer Hijacking Drives Oncogenic BCL11B Expression in Lineage-Ambiguous Stem Cell Leukemia. *Cancer Discov* **11**, 2846-2867 (2021).

https://doi.org:10.1158/2159-8290.CD-21-0145

14. Gou, P. & Zhang, W. Protein lysine acetyltransferase CBP/p300: A promising target for small molecules in cancer treatment. *Biomed Pharmacother* **171**, 116130 (2024). https://doi.org:10.1016/j.biopha.2024.116130
15. Shorstova, T., Foulkes, W. D. & Witcher, M. Achieving clinical success with BET inhibitors as anti-cancer agents. *Br J Cancer* **124**, 1478-1490 (2021). https://doi.org:10.1038/s41416-021-01321-0
16. Creasey, T. *et al.* Genetic and genomic analysis of acute lymphoblastic leukemia in older adults reveals a distinct profile of abnormalities: analysis of 210 patients from the UKALL14 and UKALL60+ clinical trials. *Haematologica* **107**, 2051-2063 (2022). https://doi.org:10.3324/haematol.2021.279177
17. Foa, R. *et al.* Long-Term Results of the Dasatinib-Blinatumomab Protocol for Adult Philadelphia-Positive ALL. *J Clin Oncol* **42**, 881-885 (2024). https://doi.org:10.1200/JCO.23.01075
18. Sawyers, C. L. The role of myc in transformation by BCR-ABL. *Leuk Lymphoma* **11 Suppl 1**, 45-46 (1993). https://doi.org:10.3109/10428199309047862
19. Sharma, N. *et al.* BCR/ABL1 and BCR are under the transcriptional control of the MYC oncogene. *Mol Cancer* **14**, 132 (2015). https://doi.org:10.1186/s12943-015-0407-0
20. Minieri, V. *et al.* Targeting STAT5 or STAT5-Regulated Pathways Suppresses Leukemogenesis of Ph+ Acute Lymphoblastic Leukemia. *Cancer Res* **78**, 5793-5807 (2018). https://doi.org:10.1158/0008-5472.CAN-18-0195
21. Shojaee, S. *et al.* Erk Negative Feedback Control Enables Pre-B Cell Transformation and Represents a Therapeutic Target in Acute Lymphoblastic Leukemia. *Cancer Cell* **28**, 114-128 (2015). https://doi.org:10.1016/j.ccell.2015.05.008
22. Kharabi Masouleh, B. *et al.* Mechanistic rationale for targeting the unfolded protein response in pre-B acute lymphoblastic leukemia. *Proc Natl Acad Sci U S A* **111**, E2219-2228 (2014). https://doi.org:10.1073/pnas.1400958111
23. Sanchez-Garcia, I. & Grutz, G. Tumorigenic activity of the BCR-ABL oncogenes is mediated by BCL2. *Proc Natl Acad Sci U S A* **92**, 5287-5291 (1995). https://doi.org:10.1073/pnas.92.12.5287
24. Sanchez-Garcia, I. & Martin-Zanca, D. Regulation of Bcl-2 gene expression by BCR-ABL is mediated by Ras. *J Mol Biol* **267**, 225-228 (1997). https://doi.org:10.1006/jmbi.1996.0779
25. de Groot, R. P., Raaijmakers, J. A., Lammers, J. W. & Koenderman, L. STAT5-Dependent CyclinD1 and Bcl-xL expression in Bcr-Abl-transformed cells. *Mol Cell Biol Res Commun* **3**, 299-305 (2000). https://doi.org:10.1006/mcbr.2000.0231
26. Dumon, S. *et al.* IL-3 dependent regulation of Bcl-xL gene expression by STAT5 in a bone marrow derived cell line. *Oncogene* **18**, 4191-4199 (1999). https://doi.org:10.1038/sj.onc.1202796
27. Gesbert, F. & Griffin, J. D. Bcr/Abl activates transcription of the Bcl-X gene through STAT5. *Blood* **96**, 2269-2276 (2000).

28. Frank, D. A. & Varticovski, L. BCR/abl leads to the constitutive activation of Stat proteins, and shares an epitope with tyrosine phosphorylated Stats. *Leukemia* **10**, 1724-1730 (1996).
29. Carlesso, N., Frank, D. A. & Griffin, J. D. Tyrosyl phosphorylation and DNA binding activity of signal transducers and activators of transcription (STAT) proteins in hematopoietic cell lines transformed by Bcr/Abl. *J Exp Med* **183**, 811-820 (1996). https://doi.org:10.1084/jem.183.3.811
30. Ilaria, R. L., Jr. & Van Etten, R. A. P210 and P190(BCR/ABL) induce the tyrosine phosphorylation and DNA binding activity of multiple specific STAT family members. *J Biol Chem* **271**, 31704-31710 (1996). https://doi.org:10.1074/jbc.271.49.31704
31. Hoelbl, A. *et al.* Stat5 is indispensable for the maintenance of bcr/abl-positive leukaemia. *EMBO Mol Med* **2**, 98-110 (2010). https://doi.org:10.1002/emmm.201000062
32. Kollmann, S. *et al.* Twins with different personalities: STAT5B-but not STAT5A-has a key role in BCR/ABL-induced leukemia. *Leukemia* **33**, 1583-1597 (2019). https://doi.org:10.1038/s41375-018-0369-5
33. Nayak, R. C. *et al.* The signaling axis atypical protein kinase C lambda/iota-Satb2 mediates leukemic transformation of B-cell progenitors. *Nat Commun* **10**, 46 (2019). https://doi.org:10.1038/s41467-018-07846-y
34. De Dominici, M. *et al.* Targeting CDK6 and BCL2 Exploits the "MYB Addiction" of Ph(+) Acute Lymphoblastic Leukemia. *Cancer Res* **78**, 1097-1109 (2018). https://doi.org:10.1158/0008-5472.CAN-17-2644
35. Menzl, I. *et al.* A kinase-independent role for CDK8 in BCR-ABL1(+) leukemia. *Nat Commun* **10**, 4741 (2019). https://doi.org:10.1038/s41467-019-12656-x
36. Buchner, M. *et al.* Identification of FOXM1 as a therapeutic target in B-cell lineage acute lymphoblastic leukaemia. *Nat Commun* **6**, 6471 (2015). https://doi.org:10.1038/ncomms7471
37. Behrens, K. *et al.* ERG and c-MYC regulate a critical gene network in BCR::ABL1-driven B cell acute lymphoblastic leukemia. *Sci Adv* **10**, eadj8803 (2024). https://doi.org:10.1126/sciadv.adj8803
38. Pfeifer, M. *et al.* SSB1/SSB2 Proteins Safeguard B Cell Development by Protecting the Genomes of B Cell Precursors. *J Immunol* **202**, 3423-3433 (2019). https://doi.org:10.4049/jimmunol.1801618
39. Boulianne, B. *et al.* Lineage-Specific Genes Are Prominent DNA Damage Hotspots during Leukemic Transformation of B Cell Precursors. *Cell Rep* **18**, 1687-1698 (2017). https://doi.org:10.1016/j.celrep.2017.01.057
40. Ng, H. L. *et al.* Promoter-centred chromatin interactions associated with EVI1 expression in EVI1+3q- myeloid leukaemia cells. *Br J Haematol* **204**, 945-958 (2024). https://doi.org:10.1111/bjh.19322
41. Schoenfelder, S., Javierre, B. M., Furlan-Magaril, M., Wingett, S. W. & Fraser, P. Promoter Capture Hi-C: High-resolution, Genome-wide Profiling of Promoter Interactions. *J Vis Exp* (2018). https://doi.org:10.3791/57320
42. Abdelrasoul, H. *et al.* Synergism between IL7R and CXCR4 drives BCR-ABL induced transformation in Philadelphia chromosome-positive acute lymphoblastic leukemia. *Nat Commun* **11**, 3194 (2020). https://doi.org:10.1038/s41467-020-16927-w

43. Creyghton, M. P. *et al.* Histone H3K27ac separates active from poised enhancers and predicts developmental state. *Proc Natl Acad Sci U S A* **107**, 21931-21936 (2010). https://doi.org:10.1073/pnas.1016071107
44. Klein, F. *et al.* The BCR-ABL1 kinase bypasses selection for the expression of a pre-B cell receptor in pre-B acute lymphoblastic leukemia cells. *J Exp Med* **199**, 673-685 (2004). https://doi.org:10.1084/jem.20031637
45. Mifsud, B. *et al.* Mapping long-range promoter contacts in human cells with high-resolution capture Hi-C. *Nat Genet* **47**, 598-606 (2015). https://doi.org:10.1038/ng.3286
46. Freire-Pritchett, P. *et al.* Global reorganisation of cis-regulatory units upon lineage commitment of human embryonic stem cells. *Elife* **6** (2017). https://doi.org:10.7554/eLife.21926
47. Alvarez-Benayas, J. *et al.* Chromatin-based, in cis and in trans regulatory rewiring underpins distinct oncogenic transcriptomes in multiple myeloma. *Nat Commun* **12**, 5450 (2021). https://doi.org:10.1038/s41467-021-25704-2
48. Gillinder, K. R. *et al.* Direct targets of pSTAT5 signalling in erythropoiesis. *PLoS One* **12**, e0180922 (2017). https://doi.org:10.1371/journal.pone.0180922
49. Godfrey, L. *et al.* MLL-AF4 binds directly to a BCL-2 specific enhancer and modulates H3K27 acetylation. *Exp Hematol* **47**, 64-75 (2017). https://doi.org:10.1016/j.exphem.2016.11.003
50. Narita, T. *et al.* Enhancers are activated by p300/CBP activity-dependent PIC assembly, RNAPII recruitment, and pause release. *Mol Cell* **81**, 2166-2182 e2166 (2021). https://doi.org:10.1016/j.molcel.2021.03.008
51. Lasko, L. M. *et al.* Discovery of a selective catalytic p300/CBP inhibitor that targets lineage-specific tumours. *Nature* **550**, 128-132 (2017). https://doi.org:10.1038/nature24028
52. Sungalee, S. *et al.* Histone acetylation dynamics modulates chromatin conformation and allele-specific interactions at oncogenic loci. *Nat Genet* **53**, 650-662 (2021). https://doi.org:10.1038/s41588-021-00842-x
53. Hogg, S. J. *et al.* Targeting histone acetylation dynamics and oncogenic transcription by catalytic P300/CBP inhibition. *Mol Cell* **81**, 2183-2200 e2113 (2021). https://doi.org:10.1016/j.molcel.2021.04.015
54. Mumbach, M. R. *et al.* HiChIP: efficient and sensitive analysis of protein-directed genome architecture. *Nat Methods* **13**, 919-922 (2016). https://doi.org:10.1038/nmeth.3999
55. Klein, F. *et al.* Tracing the pre-B to immature B cell transition in human leukemia cells reveals a coordinated sequence of primary and secondary IGK gene rearrangement, IGK deletion, and IGL gene rearrangement. *J Immunol* **174**, 367-375 (2005). https://doi.org:10.4049/jimmunol.174.1.367
56. Reckel, S. *et al.* Differential signaling networks of Bcr-Abl p210 and p190 kinases in leukemia cells defined by functional proteomics. *Leukemia* **31**, 1502-1512 (2017). https://doi.org:10.1038/leu.2017.36
57. Cutler, J. A. *et al.* Differential signaling through p190 and p210 BCR-ABL fusion proteins revealed by interactome and phosphoproteome analysis. *Leukemia* **31**, 1513-1524 (2017).

https://doi.org:10.1038/leu.2017.61

58. Bernardini, A., Lorenzo, M., Nardini, M., Mantovani, R. & Gnesutta, N. The phosphorylatable Ser320 of NF-YA is involved in DNA binding of the NF-Y trimer. *FASEB J* **33**, 4790-4801 (2019). https://doi.org:10.1096/fj.201801989R
59. Pfitzner, E., Jahne, R., Wissler, M., Stoecklin, E. & Groner, B. p300/CREB-binding protein enhances the prolactin-mediated transcriptional induction through direct interaction with the transactivation domain of Stat5, but does not participate in the Stat5-mediated suppression of the glucocorticoid response. *Mol Endocrinol* **12**, 1582-1593 (1998). https://doi.org:10.1210/mend.12.10.0180
60. Li, P. *et al.* STAT5-mediated chromatin interactions in superenhancers activate IL-2 highly inducible genes: Functional dissection of the Il2ra gene locus. *Proc Natl Acad Sci U S A* **114**, 12111-12119 (2017). https://doi.org:10.1073/pnas.1714019114
61. Katerndahl, C. D. S. *et al.* Antagonism of B cell enhancer networks by STAT5 drives leukemia and poor patient survival. *Nat Immunol* **18**, 694-704 (2017). https://doi.org:10.1038/ni.3716
62. Nabet, B. *et al.* The dTAG system for immediate and target-specific protein degradation. *Nat Chem Biol* **14**, 431-441 (2018). https://doi.org:10.1038/s41589-018-0021-8
63. Nabet, B. *et al.* Rapid and direct control of target protein levels with VHL-recruiting dTAG molecules. *Nat Commun* **11**, 4687 (2020). https://doi.org:10.1038/s41467-020-18377-w
64. Kaneshige, A. *et al.* A selective small-molecule STAT5 PROTAC degrader capable of achieving tumor regression in vivo. *Nat Chem Biol* **19**, 703-711 (2023). https://doi.org:10.1038/s41589-022-01248-4
65. Walker, S. R., Nelson, E. A. & Frank, D. A. STAT5 represses BCL6 expression by binding to a regulatory region frequently mutated in lymphomas. *Oncogene* **26**, 224-233 (2007). https://doi.org:10.1038/sj.onc.1209775
66. Wingelhofer, B. *et al.* Implications of STAT3 and STAT5 signaling on gene regulation and chromatin remodeling in hematopoietic cancer. *Leukemia* **32**, 1713-1726 (2018). https://doi.org:10.1038/s41375-018-0117-x
67. Vannam, R. *et al.* Targeted degradation of the enhancer lysine acetyltransferases CBP and p300. *Cell Chem Biol* **28**, 503-514 e512 (2021). https://doi.org:10.1016/j.chembiol.2020.12.004
68. Meyers, R. M. *et al.* Computational correction of copy number effect improves specificity of CRISPR-Cas9 essentiality screens in cancer cells. *Nat Genet* **49**, 1779-1784 (2017). https://doi.org:10.1038/ng.3984
69. Wang, X. *et al.* Genome-wide detection of enhancer-hijacking events from chromatin interaction data in rearranged genomes. *Nat Methods* **18**, 661-668 (2021). https://doi.org:10.1038/s41592-021-01164-w
70. Ottema, S. *et al.* The leukemic oncogene EVI1 hijacks a MYC super-enhancer by CTCF-facilitated loops. *Nat Commun* **12**, 5679 (2021). https://doi.org:10.1038/s41467-021-25862-3
71. Mortenson, K. L. *et al.* 3D genomic analysis reveals novel enhancer-hijacking caused by complex structural alterations that drive oncogene overexpression. *Nat Commun* **15**, 6130 (2024). https://doi.org:10.1038/s41467-024-50387-w

72. Bi, M. *et al.* Enhancer reprogramming driven by high-order assemblies of transcription factors promotes phenotypic plasticity and breast cancer endocrine resistance. *Nat Cell Biol* **22**, 701-715 (2020). https://doi.org:10.1038/s41556-020-0514-z
73. Roe, J. S. *et al.* Enhancer Reprogramming Promotes Pancreatic Cancer Metastasis. *Cell* **170**, 875-888 e820 (2017). https://doi.org:10.1016/j.cell.2017.07.007
74. Poli, V. *et al.* MYC-driven epigenetic reprogramming favors the onset of tumorigenesis by inducing a stem cell-like state. *Nat Commun* **9**, 1024 (2018). https://doi.org:10.1038/s41467-018-03264-2
75. Corleone, G. *et al.* Enhancer engagement sustains oncogenic transformation and progression of B-cell precursor acute lymphoblastic leukemia. *J Exp Clin Cancer Res* **43**, 179 (2024). https://doi.org:10.1186/s13046-024-03075-y
76. Narang, S. *et al.* Clonal evolution of the 3D chromatin landscape in patients with relapsed pediatric B-cell acute lymphoblastic leukemia. *Nat Commun* **15**, 7425 (2024). https://doi.org:10.1038/s41467-024-51492-6
77. Mullighan, C. G. *et al.* BCR-ABL1 lymphoblastic leukaemia is characterized by the deletion of Ikaros. *Nature* **453**, 110-114 (2008). https://doi.org:10.1038/nature06866
78. Hu, Y. *et al.* Superenhancer reprogramming drives a B-cell-epithelial transition and high-risk leukemia. *Genes Dev* **30**, 1971-1990 (2016). https://doi.org:10.1101/gad.283762.116
79. Lambert, S. A. *et al.* The Human Transcription Factors. *Cell* **175**, 598-599 (2018). https://doi.org:10.1016/j.cell.2018.09.045

Figures

Figure 1

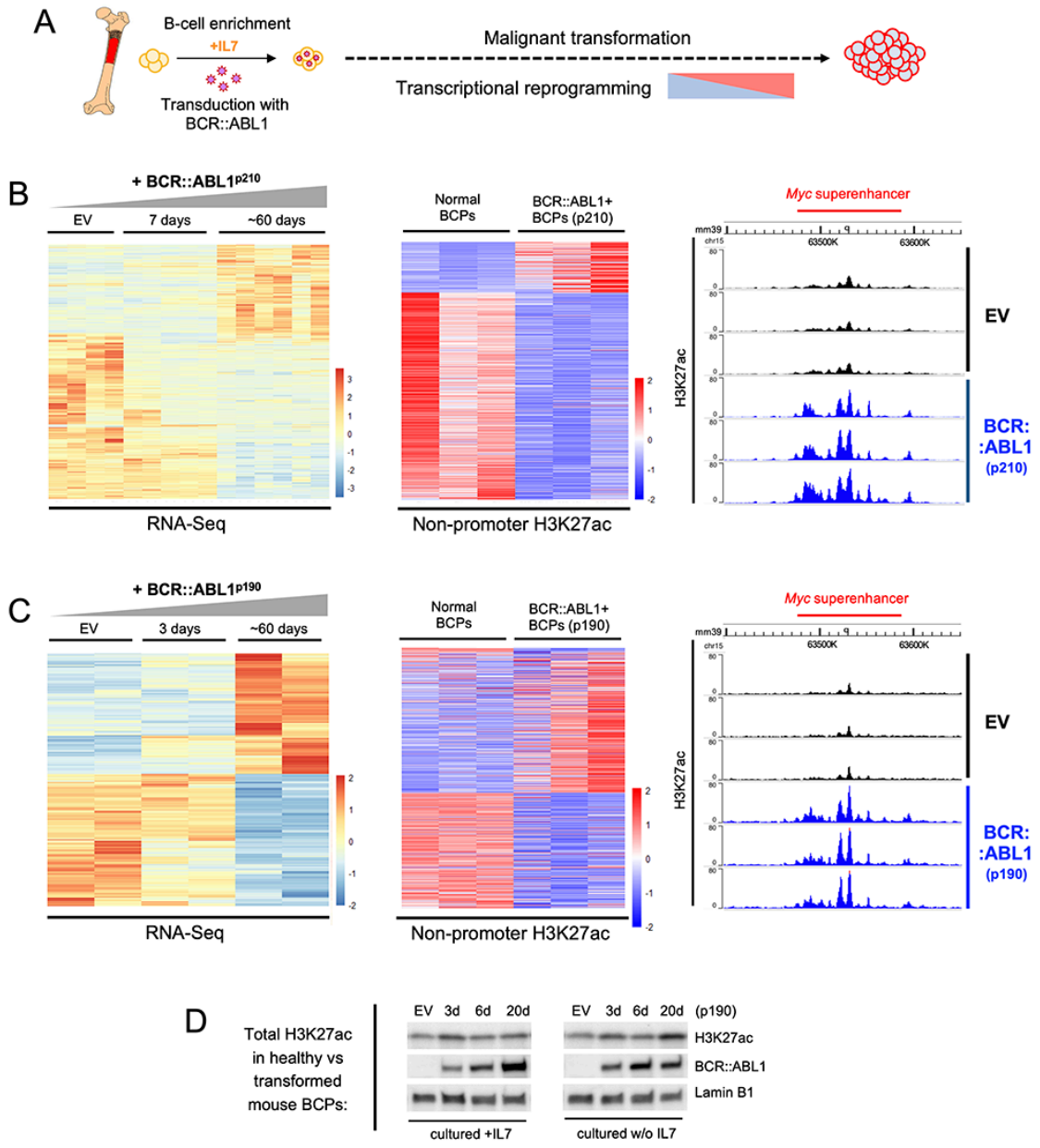

Figure 1

BCR::ABL1-induced malignant transformation is associated with H3K27ac-defined changes in enhancer activation. (A) A schematic of the experiments performed in this figure is shown. (B) (Left) A heatmap is shown visualizing differentially expressed genes (DEGs, RNA-Seq) during malignant transformation of B-cell precursors by BCR::ABL1. B-cell precursors (BCPs) isolated from *53BP1-/-* mice for this experiment were transduced with either MIGR1 empty vectors (EV) or BCR::ABL1(p210) vectors and analyzed 7 days

post transduction. BCR::ABL1 transduced cells were additionally analyzed at ~60 days. (Middle) Normal BCPs (EV) and fully transformed BCPs (~60d BCR::ABL1) were further assessed by H3K27ac ChIP-Seq, and differential H3K27ac signals at non-promoter locations are shown in this heatmap. (Right) Custom tracks of differential H3K27ac signals at the *Myc* super-enhancer in BCR::ABL1(p210) expressing cells are shown as an example. (C) (Left) A heatmap is shown visualizing differentially expressed genes (DEGs, RNA-Seq) during malignant transformation of B-cell precursors by BCR::ABL1 but using BCPs isolated from C57BL/6 mice and with BCR::ABL1(p190). (Middle) Differential H3K27ac signals at non-promoter locations for normal and fully transformed BCPs are shown. (Right) Custom tracks of differential H3K27ac signals at the *Myc* super-enhancer in BCR::ABL1(p190) expressing cells are shown as an example as in (B). (D) Total H3K27ac signals during malignant transformation of murine B-cell precursors from C57BL/6 mice by BCR::ABL1(p190) were analyzed by Western Blot. BCR::ABL1^{p190} was visualized using a BCR antibody, Lamin B1 was blotted as loading control.

Figure 2

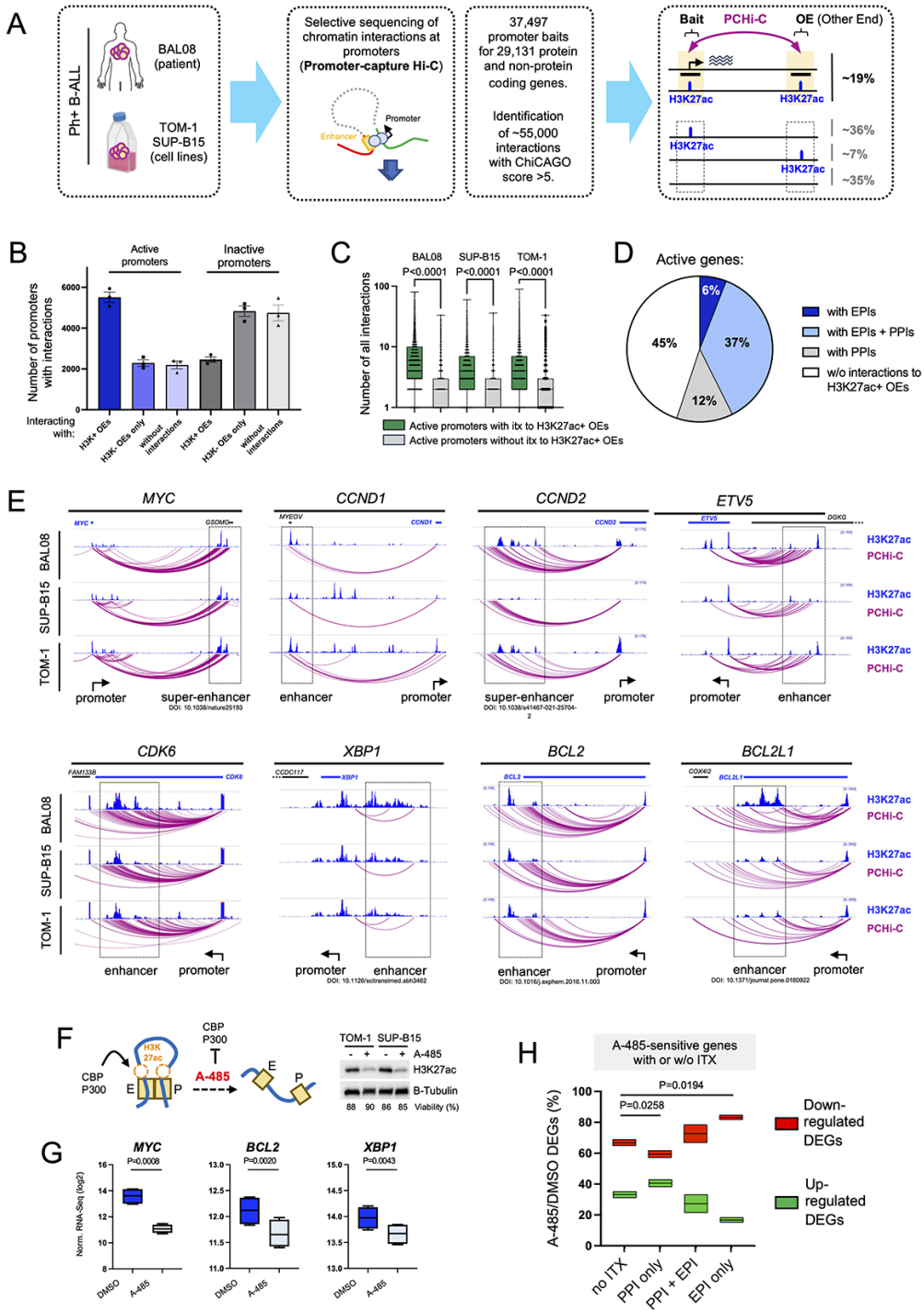

Figure 2

Key genes for Ph+B-ALL cells are connected to enhancers through long-range chromatin interactions. (A) Schematic of the analysis of enhancer-promoter interactions in Ph+B-ALL cells by Promoter-Capture Hi-C (PCHi-C) and H3K27ac ChIP-Seq. The window on the right depicts potential chromatin interactions detected in this approach, with interactions of an active promoter with an active (H3K27ac+) other end (OE) representing ~19% of all interactions. (B) Bar chart showing the number of active versus inactive

promoters with PCHi-C interactions that do or do not display interactions with at least one H3K27ac+ OE (i.e., H3K+ OE vs H3K- OE) and promoters without PCHi-C-defined interactions. Individual dots represent numbers obtained for the three samples analyzed by PCHi-C (i.e., BAL08, SUP-B15, TOM-1). (C) Box plot showing the total numbers of interactions for active promoters that do or do not display interactions (itx) with at least one H3K27ac+ OE (i.e., H3K+ OE vs H3K- OE). Number of interactions include promoter interactions without H3K27ac+ OEs. Statistical analysis was performed using GraphPad PRISM unpaired Student's t-test. (D) A pie chart is shown, indicating the average percentage of active genes in Ph+B-ALL cells with EPIs only, EPIs+PPIs, PPIs only, or without interactions to H3K27ac+ OEs. (E) Arc plots and custom tracks visualizing PCHi-C-defined chromatin interactions and H3K27ac signals at active enhancers and promoters (i.e., EPIs) for selected genes with described key functions for Ph+B-ALL cells are shown. Custom tracks were generated using the WashU epigenome browser and only interactions that start and end in the depicted area are shown. (F-H) The enhancer activator CBP/P300[50] was inhibited in Ph+B-ALL cells with sub-lethal concentrations of A-485[51] and resulting changes in gene expression were monitored by RNA-Seq and compared to promoter-enhancer interactions defined by PCHi-C. (F) A schematic is shown summarizing work from Sungalee et al[52] demonstrating that A-485 interferes with enhancer function at least in part by reducing their interaction with promoters. (Right) A Western blot is shown confirming the inhibitory function of A-485 (48 h with 0.5 mM) on the enzymatic function of CBP/P300 by visualizing H3K27ac levels. Viability counts determined by Trypan blue staining are indicated below. (G) Normalized RNA-Seq values of A485-treated cells for three genes with importance in Ph+B-ALL are shown as an example (see Suppl.Fig.2H/I for further examples). (H) Percentages of upregulated and downregulated DEGs defined by RNA-Seq from the comparison of A-485 vs DMSO treatment of Ph+B-ALL cells are shown. Percentages are individually shown for genes with EPIs in comparison to genes with PPIs, genes with EPIs+PPIs, and genes with neither EPIs nor PPIs (no ITX). Data represents results obtained in TOM-1 and SUP-B15 cells (see Suppl.Fig.2J for individual results on TOM-1 and SUP-B15). Statistical analysis was performed by paired Student's t-test using Graphpad PRISM.

Figure 3

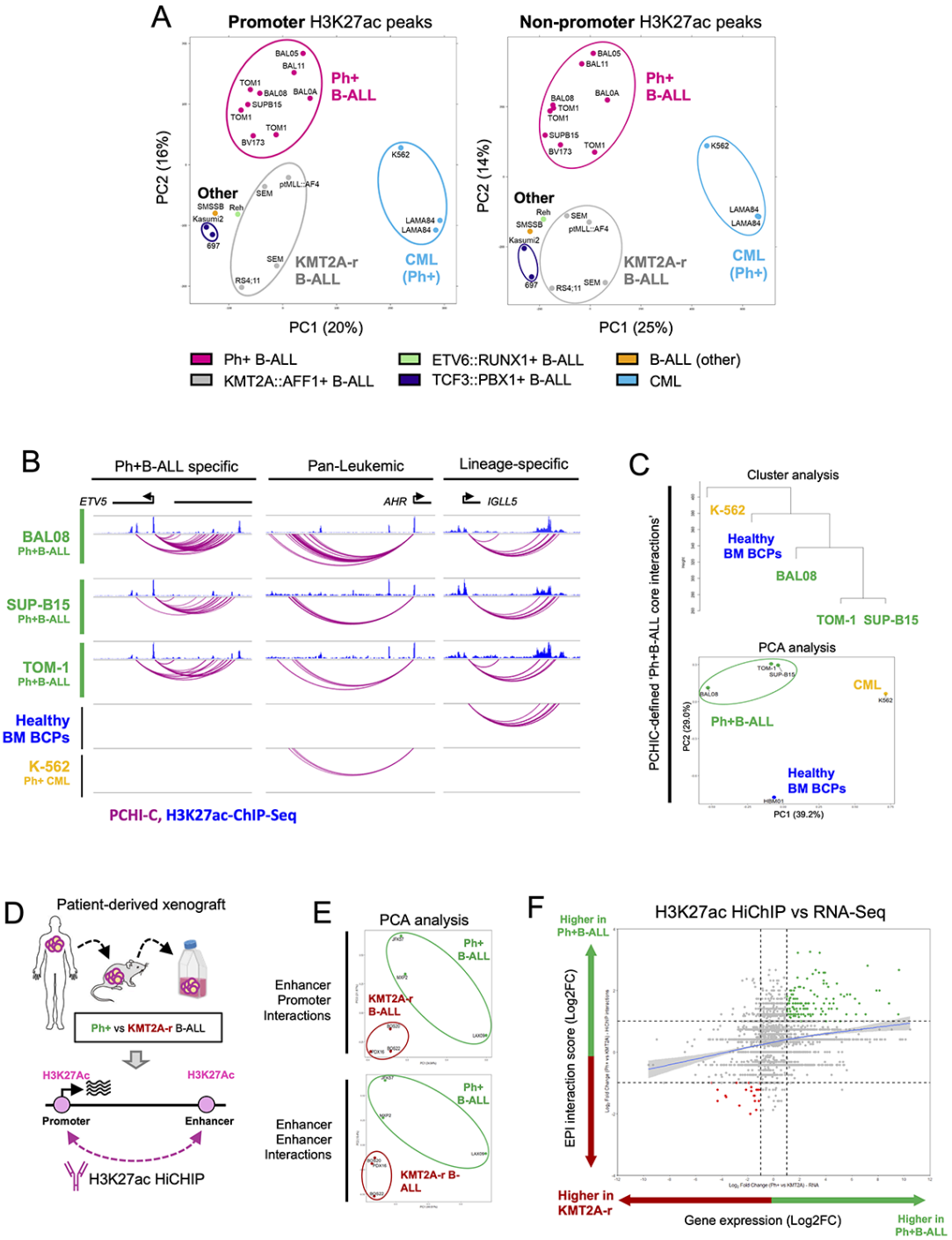

Figure 3

Enhancer-promoter interactions define Ph+B-ALL identity and mirror Ph+B-ALL-specific gene expression. (A) Principal component analysis (PCA) of H3K27ac ChIP-Seq signals from cell lines and primary leukemia cells from patients for the indicated leukemia subtypes is shown. PCA analysis was performed using exclusively H3K27ac signals at promoters (left) or at non-promoter regions (right). Leukemia subtypes of cell lines were defined using cytogenetic and phenotypic data from DSMZ. Data on

KMT2A::AFF1+ B-ALL cells, including ptMLL::AF4 were obtained from GSE74812, GSE71616 & GSE135024, while data on Ph+B-ALLs (i.e., BAL0A, BAL05, BAL08, BAL11) was generated by this study. (B) Arc plots of PCHi-C interactions are shown for genes that show leukemia- and/or lineage-specific PCHi-C interactions. PCHi-C data on three Ph+B-ALL samples (BAL08 = patient, TOM-1/SUP-B15 = cell lines), and from healthy B-cell precursors (BCPs) as well as Ph+ myeloid leukemia cells (K562) is shown. H3K27ac ChIP-Seq custom tracks are added where available. Custom tracks were generated using the WashU epigenome browser and only interactions that start and end in the depicted area are shown. (C) A cluster dendrogram (top) and PCA plot (bottom) is shown using 'Ph+B-ALL CORE interactions' that allow separation of Ph+B-ALL cells from healthy BCPs and Ph+ myeloid leukemia cells. (D) A summary of the H3K27ac HiChIP experiment is shown. (E) PCA plots are shown for H3K27ac HiChIP defined enhancer-promoter interactions (EPIs, top) and enhancer-enhancer interactions (EEIs) for PDX-derived Ph+ (n=3) and *KMT2A::AFF1* (n=3) B-ALL cells. (F) A comparison of H3K27ac HiChIP defined EPIs and respective gene expression is shown, using log2FC values of EPIs per gene versus the expression of the respective genes for Ph+B-ALL compared to *KMT2A::AFF1*+ B-ALL. B-ALL patient data from the TARGET study[1] was used for patient-specific gene expression.

Figure 4

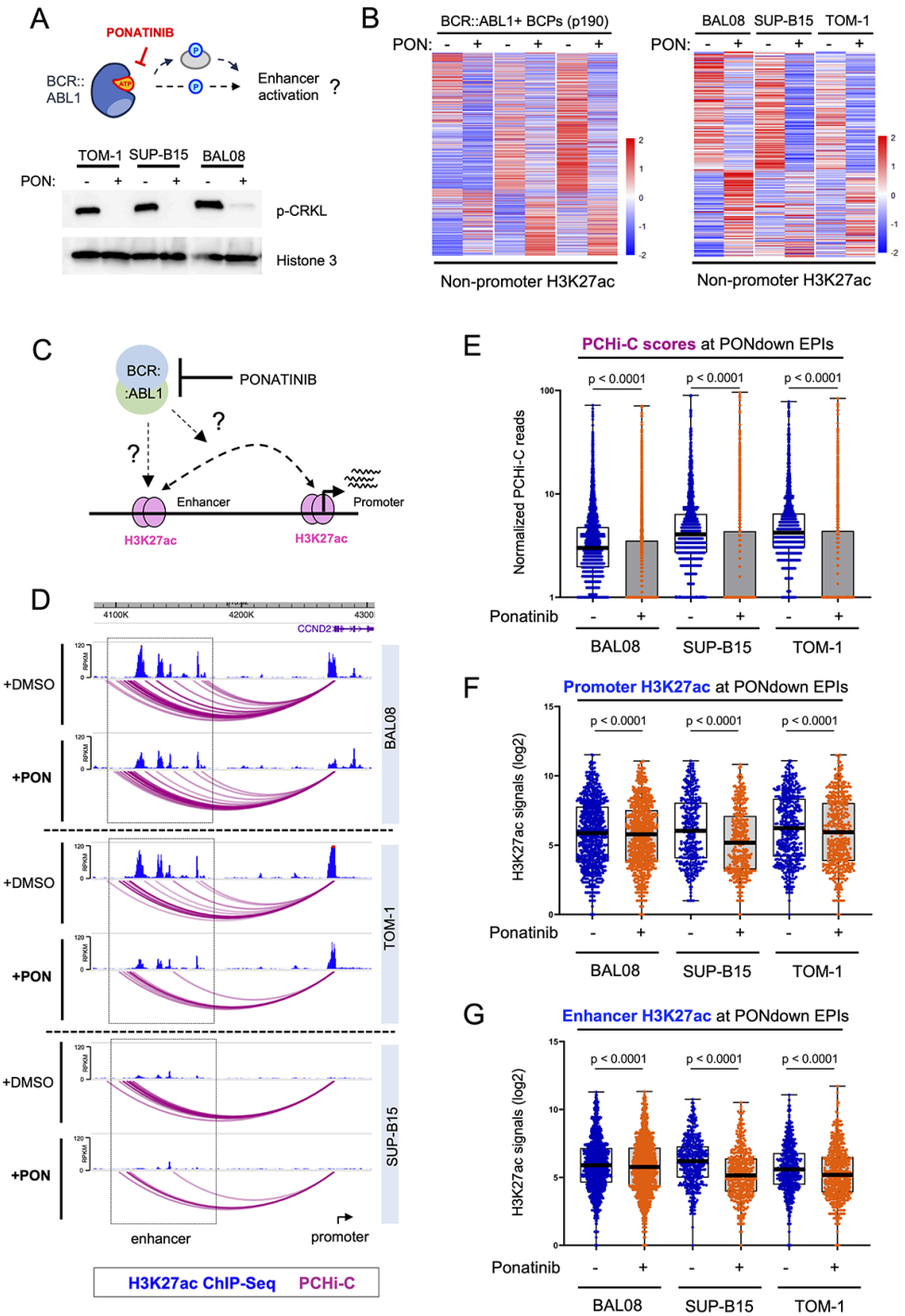

Figure 4

Enhancer activity and enhancer-promoter interactions of BCR::ABL1-induced genes depend on BCR::ABL1 kinase activity. (A) (Top) A schematic to demonstrate the mechanism of action of Ponatinib is shown. (Bottom) A Western blot to validate the effectiveness of 24 h 0.1 mM Ponatinib treatment to inhibit BCR::ABL1 activity in Ph+B-ALL cells is shown using the historic BCR::ABL1 target CRKL. (B) Heatmaps of H3K27ac ChIP-Seq signals at non-promoter regions are shown for DMSO- versus

Ponatinib-treated murine (left) and human (right) BCR::ABL1^{p190}-driven B-ALL cells. Only regions with differential H3K27ac signals are shown. (C) A schematic summarizing the analysis of EPIs and H3K27ac ChIP-Seq signals at Ponatinib-sensitive, downregulated genes with EPIs is performed for D-G is shown. (D) Arc plots of PCHi-C and H3K27ac ChIP-Seq signals are shown for the known BCR::ABL1-deregulated gene, *CCND2*. Data is shown for three Ph+B-ALL samples (BAL08, SUP-B15 and TOM-1) treated with Ponatinib or DMSO as control. (E) PCHi-C scores of EPIs at Ponatinib-sensitive, downregulated genes with EPIs are shown. (F) H3K27ac ChIP-Seq signals at promoters of Ponatinib-sensitive, downregulated genes with EPIs are shown. (G) H3K27ac ChIP-Seq signals at enhancer regions of Ponatinib-sensitive, downregulated genes with EPIs are shown. Statistical analysis in E-G was performed by paired Student's t-test on GraphPad PRISM.

Figure 5

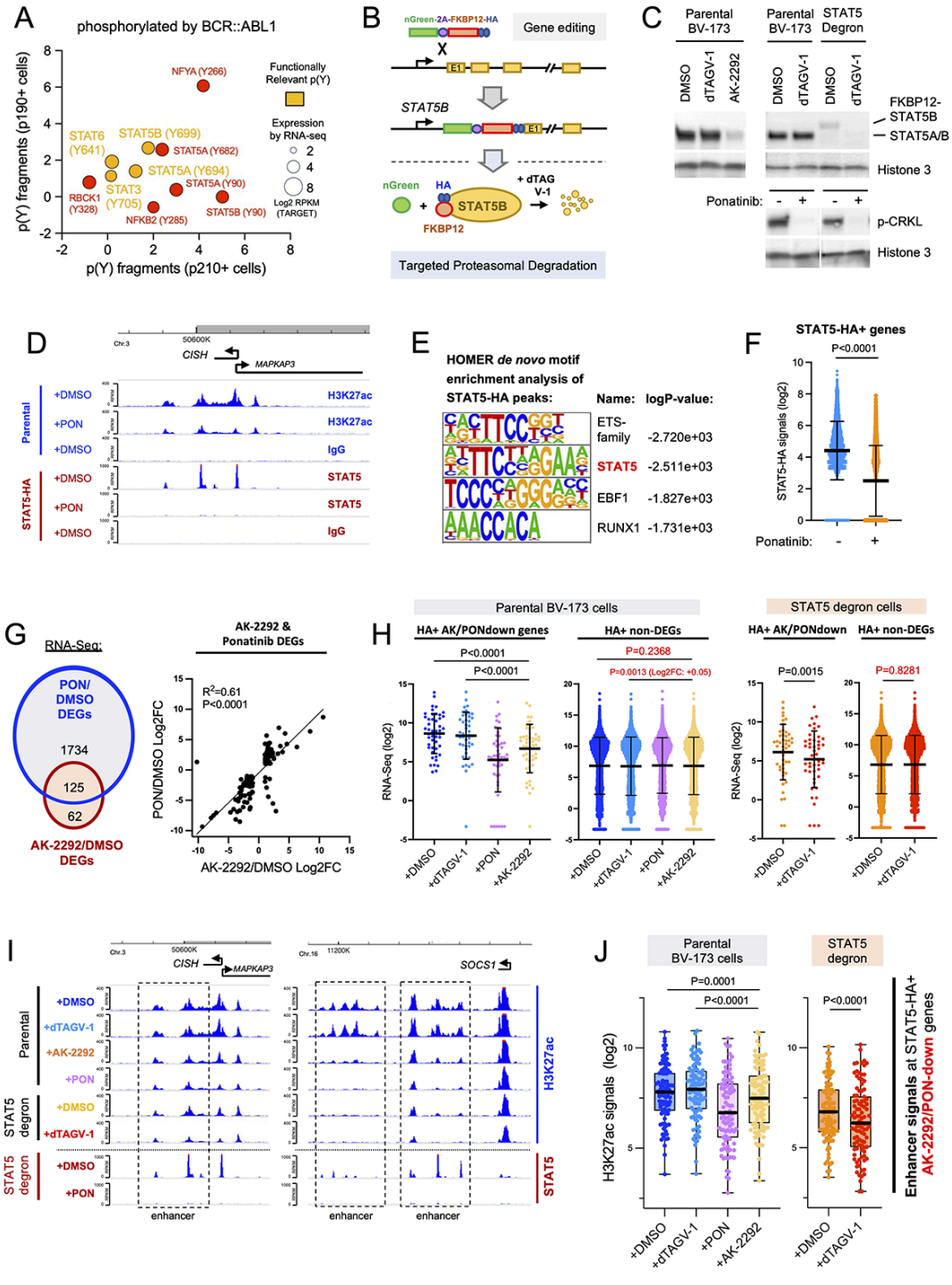

Figure 5

BCR::ABL1 induces enhancer activation in part through the BCR::ABL1-induced transcription factor STAT5. (A) An XY plot is shown visualizing BCR::ABL1-phosphorylated TFs identified by two published mass spectrometry data sets[56,57]. X and Y axes indicate the p210/parental and p190/parental median normalized ratios from Cutler et al. TFs from these datasets were identified using a previously published list of human TF-encoding genes[79]. Dot sizes indicate the relative expression of the relative genes in

Ph+B-ALL cells using RNA-Seq data from the TARGET study. Previously reported functionally relevant phospho-tyrosines (pY) are highlighted. Note that NFYA (Y266) is functionally irrelevant as described by Bernardini et al[58]. (B) A schematic of the gene targeting strategy and mechanism of action of the degron/dTAG model used here is shown. (C) Representative Western blots of parental or STAT5-degron BV-173 Ph+B-ALL cells are shown. (Left) Parental BV-173 were treated with 2.5 mM AK-2292 (targeting STAT5A/B), 0.25 mM dTAGV-1 (non-targeting degrader control), or DMSO (1:1000) for 48 h and blotted for total STAT5A/B protein. (Right) Parental and STAT5-degron BV-173 cells were treated with 0.25 mM dTAGV-1 or DMSO (1:1000) for 48 h and blotted for total STAT5A/B. Note that the $FKBP12^{F36V}$ and HA-tag addition to STAT5B in STAT5-degron cells increases the protein size of STAT5B from 90 kDa to 102 kDa. (Bottom) Parental and STAT5-degron BV-173 cells were treated with Ponatinib, or DMSO as control, for 48 h and blotted for p-CRKL. Histone 3 was visualized as loading control for all blots. (D) Custom tracks are shown visualizing H3K27ac and STAT5-HA ChIP-Seq signals at the canonical STAT5 target gene *CISH* for parental and STAT5-degron BV-173 cells treated with Ponatinib, or DMSO as control, for 48 h. ChIP-Seq using isotype control IgG was performed as a control for the antibodies used. (E) DNA-binding motifs and enrichment p-values of the top four most-enriched TFs at STAT5-HA ChIP-Seq peaks are shown. (F) A bar diagram of STAT5-HA signals at STAT5-HA-bound promoters in STAT5-degron BV-173 cells treated for 48 h with Ponatinib, or DMSO as control, is shown. Statistics were performed using GraphPad PRISM and paired Student's t-test. (G) (Left) A Venn diagram visualizing the overlap of differentially expressed genes (DEGs) for the comparisons Ponatinib/DMSO and AK-2292/DMSO of parental BV-173 cells is shown. (Right) An XY plot of the 125 genes that are DEGs for both, Ponatinib/DMSO and AK-2292/DMSO, is shown depicting the respective $\log_2$ fold change (Log2FC) values for each comparison. (H) Bar diagrams showing the normalized RNA-Seq counts of genes that are STAT5-HA-bound and downregulated by both Ponatinib and AK-2292, or of STAT5-HA-bound genes that are not Ponatinib/AK-2292 sensitive. Results are shown for parental or STAT5-degron BV-173 cells treated as indicated for 48 h. Statistics were performed using GraphPad PRISM and paired Student's t-test. (I) Custom tracks are shown that visualize H3K27ac and STAT5-HA ChIP-Seq signals at the canonical STAT5 target genes *CISH* and *SOCS1* for parental and STAT5-degron BV-173 cells treated for 48 h as indicated. (J) Bar diagrams showing total H3K27ac signals at STAT5-HA-bound non-promoter (enhancer) regions in a 50 kb vicinity of promoters from STAT5-HA-bound genes that are downregulated by both AK-2292 and Ponatinib. Analysis was performed for parental and STAT5-degron BV-173 cells treated for 48 h as indicated. Statistics were performed using GraphPad PRISM and paired Student's t-test.

Figure 6

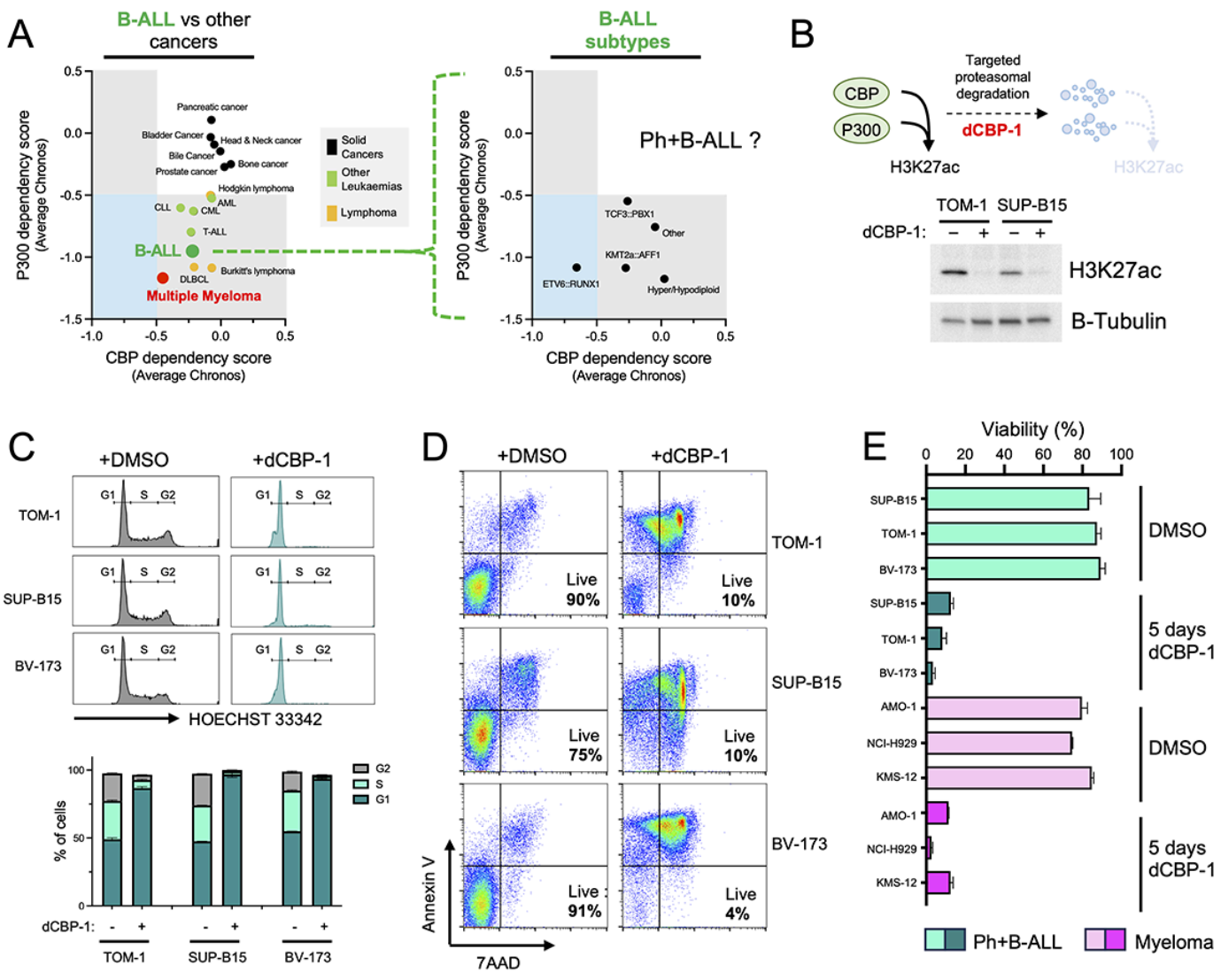

Figure 6

Interference with enhancer function causes cell-cycle arrest and apoptosis in Ph+B-ALL cells. (A) XY plots of DepMap data showing average dependency scores (Chronos) for P300 and CBP for leukemia and lymphoma cells, and for CBP/P300 inhibition insensitive solid cancers for comparison. Areas of dependency (Chronos scores <-0.5) are highlighted in grey (single dependency) or blue shade (dependency for both, CBP and P300). (Left) A comparison of different leukemia and lymphoma types is shown with non-hematological cancers as indicated for comparison. (Right) An analysis focusing on B-ALL subtypes is shown. Note that Ph+B-ALL is not represented by DepMap. (B) (Top) A schematic of mechanism of action of the CBP/P300 PROTAC dCBP-1 is shown. (Bottom) Western blot validation of dCBP-1 treatment of two Ph+B-ALL cell lines (48 h, 0.25 mM) using H3K27ac as read-out. DMSO

treatment was performed as control. (C) Cell-cycle analysis of 48 h dCBP-1 treated Ph+B-ALL cells (n=2) by HOECHST 33342 staining. (Top) Representative histograms are shown indicating cells in G1, S and G2 phase of the cell cycle. (Bottom) Bar diagram summarizing the results of two experiments. (D) Viability analysis of Ph+B-ALL cells treated for 5 days with 0.25 mM dCBP-1 using 7AAD/Annexin V staining. Representative flow cytometry dot plots are shown with live cell percentages indicated (7AAD-/Annexin V- cells, lower left quadrant). (E) A bar diagram is shown summarizing the results of 5-day dCBP-1 treatments of Ph+B-ALL cells (n=3). MM cells were treated for comparison. Cell line names are indicated in the figure.

Supplementary Files

This is a list of supplementary files associated with this preprint. Click to download.

- Ngetal2024SupplementaryInformationSuppl.FiguresandMethods18.10.24FINALforsubmission.pdf